High-speed imaging of human retina *in vivo* with swept-source optical coherence tomography

H. Lim, M. Mujat, C. Kerbage, E. C. W. Lee, and Y. Chen

Harvard Medical School and Wellman Center for Photomedicine, Massachusetts General Hospital
50 Blossom Street, Boston, Massachusetts 02114

Teresa C. Chen

Massachusetts Eye and Ear Infirmary and Harvard Medical School, 243 Charles Street, Boston, Massachusetts 02114

J. F. de Boer

Harvard Medical School and Wellman Center for Photomedicine, Massachusetts General Hospital
50 Blossom Street, Boston, Massachusetts 02114
deboer@helix.mgh.harvard.edu

Abstract: We present the first demonstration of human retinal imaging *in vivo* using optical frequency domain imaging (OFDI) in the 800-nm range. With 460-μW incident power on the eye, the sensitivity is 91 dB at maximum and >85 dB over 2-mm depth range. The axial resolution is 13 μm in air. We acquired images of retina at 43,200 depth profiles per second and a continuous acquisition speed of 84 frames/s (512 A-lines per frame) could be maintained over more than 2 seconds.

OCIS codes: (110.4500) Optical coherence tomography; (120.3180) Interferometry; (140.3600) Lasers, tunable; (170.3880) Medical and biological imaging; (170.4470) Ophthalmology; (330.4460) Ophthalmic optics

References and links

1. D. Huang, E. A. Swanson, C. P. Lin, J. S. Schuman, W. G. Stinson, W. Chang, M. R. Hee, T. Flotte, K. Gregory, C. A. Puliafito, and J. G. Fujimoto, "Optical coherence tomography," Science **254**, 1178-1181 (1991).
2. M. R. Hee, J. A. Izatt, E. A. Swanson, D. Huang, J. S. Schuman, C. P. Lin, C. A. Puliafito, and J. G. Fujimoto, "Optical coherence tomography of the human retina," Archives of Ophthalmology **113**, 325-32 (1995).
3. W. Drexler, "Ultrahigh-resolution optical coherence tomography," J Biomed Opt **9**, 47-74 (2004).
4. M. Wojtkowski, R. Leitgeb, A. Kowalczyk, T. Bajraszewski, and A. F. Fercher, "In vivo human retinal imaging by fourier domain optical coherence tomography," J. Biomed. Opt. **7**, 457-463 (2002).
5. N. Nassif, B. Cense, B. Hyle Park, S. H. Yun, T. C. Chen, B. E. Bouma, G. J. Tearney, and J. F. de Boer, "In vivo human retinal imaging by ultrahigh-speed spectral domain optical coherence tomography," Opt. Lett. **29**, 480-482 (2004).
6. N. Nassif, B. Cense, B. Park, M. Pierce, S. Yun, B. Bouma, G. Tearney, T. Chen, and J. de Boer, "In vivo high-resolution video-rate spectral-domain optical coherence tomography of the human retina and optic nerve," Opt. Express **12**, 367-376 (2004).
7. T. Mitsui, "Dynamic range of optical reflectometry with spectral interferometry," Jpn. J. Appl. Phys. **38,** 6133-6137 (1999).
8. R. Leitgeb, C. Hitzenberger, and A. Fercher, "Performance of fourier domain vs. time domain optical coherence tomography," Opt. Express **11**, 889-894 (2003).
9. J. F. de Boer, B. Cense, B. H. Park, M. C. Pierce, G. J. Tearney, and B. E. Bouma, "Improved signal-to-noise ratio in spectral-domain compared with time-domain optical coherence tomography ," Opt. Lett. **28**, 2067-2069 (2003).
10. M. A. Choma, M. V. Sarunic, C. H. Yang, and J. A. Izatt, "Sensitivity advantage of swept source and Fourier domain optical coherence tomography," Opt. Express **11**, 2183-2189 (2003).

#74442 - $15.00 USD Received 29 August 2006; revised 4 December 2006; accepted 5 December 2006

11. B. Cense, N. A. Nassif, T. C. Chen, M. C. Pierce, S. Yun, B. H. Park, B. E. Bouma, G. J. Tearney, and J. F. de Boer, "Ultrahigh-resolution high-speed retinal imaging using spectral-domain optical coherence tomography," Opt. Express **12**, 2435-2447 (2004).
12. M. Wojtkowski, V. Srinivasan, T. Ko, J. Fujimoto, A. Kowalczyk, and J. Duker, "Ultrahigh-resolution, high-speed, Fourier domain optical coherence tomography and methods for dispersion compensation," Opt. Express **12**, 2404-2422 (2004).
13. S. H. Yun, G. Tearney, J. de Boer, and B. Bouma, "Pulsed-source and swept-source spectral-domain optical coherence tomography with reduced motion artifacts," Opt. Express **12**, 5614-5624 (2004).
14. J. W. You, T. C. Chen, M. Mujat, B. H. Park, and J. F. de Boer, "Pulsed illumination spectral-domain optical coherence tomography for human retinal imaging," Opt. Express **14**, 6739-6748 (2006).
15. S. H. Yun, G. J. Tearney, J. F. de Boer, N. Iftimia, and B. E. Bouma, "High-speed optical frequency-domain imaging," Opt. Express **11**, 2953-2963 (2003).
16. S. R. Chinn, E. A. Swanson, and J. G. Fujimoto, "Optical coherence tomography using a frequency-tunable optical source," Opt. Lett. **22**, 340-342 (1997).
17. S. Yun, G. Tearney, B. Bouma, B. Park, and J. de Boer, "High-speed spectral-domain optical coherence tomography at 1.3 μm wavelength," Opt. Express **11**, 3598-3604 (2003).
18. Y. Yasuno, V. D. Madjarova, S. Makita, M. Akiba, A. Morosawa, C. Chong, T. Sakai, K. P. Chan, M. Itoh, and T. Yatagai, "Three-dimensional and high-speed swept-source optical coherence tomography for in vivo investigation of human anterior eye segments," Opt. Express **13**, 10652-10664 (2005).
19. E. C. W. Lee, J. F. de Boer, M. Mujat, H. Lim, and S. H. Yun, "In vivo optical frequency domain imaging of human retina and choroid," Opt. Express **14**, 4403-4411 (2006).
20. H. Lim, J. F. de Boer, B. H. Park, E. C. Lee, R. Yelin, and S. H. Yun, "Optical frequency domain imaging with a rapidly swept laser in the 815-870 nm range," Opt. Express **14**, 5937-5944 (2006).
21. S. H. Yun, C. Boudoux, G. J. Tearney, and B. E. Bouma, "High-speed wavelength-swept semiconductor laser with a polygon-scanner-based wavelength filter," Opt. Lett. **28**, 1981-1983 (2003).
22. D. B. Mortimore, "Fiber loop reflectors," J. Lightwave Technol. **7,** 1217- 1224 (1988).
23. ANSI, American National Standard for the Safe Use of Lasers, ANSI Z136.1 (Laser Institute of America, Orlando, FL, 2000).
24. J. Liang, D. R. Williams, and D. T. Miller, "Supernormal vision and high-resolution retinal imaging through adaptive optics ," J. Opt. Soc. Am. A **14**, 2884-2892 (1997).
25. A. Roorda, F. Romero-Borja, W. Donnelly, III, H. Queener, T. Hebert, and M. Campbell, "Adaptive optics scanning laser ophthalmoscopy," Opt. Express **10**, 405-412 (2002).
26. B. Hermann, E. J. Fernández, A. Unterhuber, H. Sattmann, A. F. Fercher, W. Drexler, P. M. Prieto, and P. Artal, "Adaptive-optics ultrahigh-resolution optical coherence tomography," Opt. Lett. **29**, 2142-2144 (2004).
27. Y. Zhang, B. Cense, J. Rha, R. S. Jonnal, W. Gao, R. J. Zawadzki, J. S. Werner, S. Jones, S. Olivier, and D. T. Miller, "High-speed volumetric imaging of cone photoreceptors with adaptive optics spectral-domain optical coherence tomography," Opt. Express **14**, 4380-4394 (2006).

1. Introduction

Optical coherence tomography (OCT) provides a unique means to obtain depth-resolved, high-resolution images of retina *in vivo* [1-6]. High acquisition speed is valued in most imaging applications, but particularly in ophthalmology it minimizes artifacts that arise from eye movements. 3-D volumetric scanning within a time acceptable in a clinical setting may also permit temporally resolving fast physiological processes *en masse* during visual perception.

Spectral-domain or frequency-domain OCT (SD/FD-OCT) has become the preferred method for retinal imaging owing to its high imaging speed [5, 6], enhanced signal-to-noise ratio (SNR) [7-10] and the availability of broadband sources permitting ultrahigh resolution retinal imaging [11, 12]. However, the state-of-the-art spectrometers are hampering further improvements 1) with limited detection efficiency (~25%) and 2) the obtainable spectral resolution causes approximately a 6-dB sensitivity drop over a 1-mm depth range [6]. Furthermore, rapid scanning of the probe beam in SD-OCT has the adverse effect of fringe washout, which causes SNR to decrease [13, 14].

Alternately optical frequency domain imaging (OFDI), or swept-source OCT, uses a wavelength-tuned laser [15, 16]. The method derives the spectrally resolved interference not from a spectrometer, but rather from rapidly sweeping the wavelength of a laser. Simpler detection in OFDI, *i.e.* use of a single-point photodiode instead of a spectrometer, enables higher detection efficiency, which could improve sensitivity. It has been demonstrated that the

#74442 - $15.00 USD Received 29 August 2006; revised 4 December 2006; accepted 5 December 2006

typical depth range of OFDI [15] could be longer than that of spectrometer-based SD-OCT systems [17]. Improved ranging depth can provide an important benefit in a clinical setting, where patient motion poses a challenge in keeping all retinal structures of interest within the ranging depth, such as increased cupping in optic nerve head (ONH) which is an important diagnostic signature of glaucomatous eyes. OFDI facilitates fast surveillance, which is a vital feature in clinically viable, volumetric retinal imaging. OFDI technique has been applied successfully in ophthalmic imaging to visualize anterior [18] and posterior segments [19] at 1300 and 1050 nm, respectively. Recently we have demonstrated for the first time high-speed OFDI in the 800-nm range [20] with a depth range of ~2 mm, much better compared to SD/FD-OCT systems. However, the axial resolution realized with OFDI, both at 800 [20] or 1050 nm [19], is not so impressive; ~14 μm in air, a factor of 3.5 worse than that with SD/FD-OCT systems [11, 12].

In this paper, we demonstrate 800-nm OFDI imaging of human retina *in vivo*, for the first time to the best of our knowledge. A rapidly wavelength-tuned laser in the range of 815-870 nm was a linear cavity design [19]. An eye of healthy volunteer was imaged with an A-line rate of 43.2 kHz. An axial resolution of 13-13.5 μm in air, a peak sensitivity of 91 dB and better than 85-dB sensitivities were achieved over a 2-mm depth range with a sample arm power of 460 μW.

2. Method

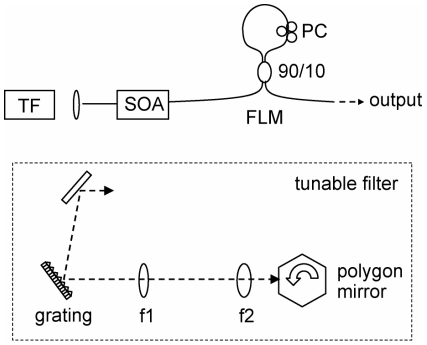

Fig. 1. Schematic of the wavelength-swept laser. TF: tunable filter, SOA: semiconductor optical amplifier, FLM: fiber loop mirror, PC: Polarization controller. The focal length f1 and f2 is 75 and 40 mm, respectively.

The wavelength-swept laser is depicted in Fig. 1. Unlike the previous ring-cavity laser that we have recently demonstrated [20], the current design of a linear cavity does not include a free-space isolator in the cavity, which is a bulky and expensive component. In addition, the easier alignment makes the laser favorable for integrated instrumentation. It consists of three elements; a wavelength tunable filter (TF), a semiconductor optical amplifier (SOA), and a fiber loop mirror (FLM). The TF was as specified earlier [20] except that the light out of the fiber was collimated with a lens (f = 11 mm) and the incident angle on the grating was 75 degrees. We estimate from these experimental parameters that the linewidth of the spectral filter is 0.07 nm [21] and the free spectral range is 54 nm. The gain medium is a commercially-available semiconductor optical amplifier (Superlum Diodes, Ltd) [20]. The injection current level was 140 mA. The fiber loop mirror was constructed with a 90/10 coupler and a fiber polarization controller, where the 90% port was directed to the output. The reflectivity of the fiber loop depends on the birefringence of the fiber and the coupling ratio. In this case, the feedback coupling ratio could be varied between 0-36% with a polarization controller [22]. Restricting the feedback coupling ratio to at most 36% helped managing the feedback power to avoid permanent damage to the SOA [20]. The cavity round trip time, measured from the mode beating noise with an electrical spectrum analyzer, was 17.5 ns. The

#74442 - $15.00 USD Received 29 August 2006; revised 4 December 2006; accepted 5 December 2006

oscilloscope trace of the laser output with a 43.2-KHz rate is shown in Fig. 2(a) and the corresponding instantaneous optical power in the reference arm is illustrated in Fig. 2(b).

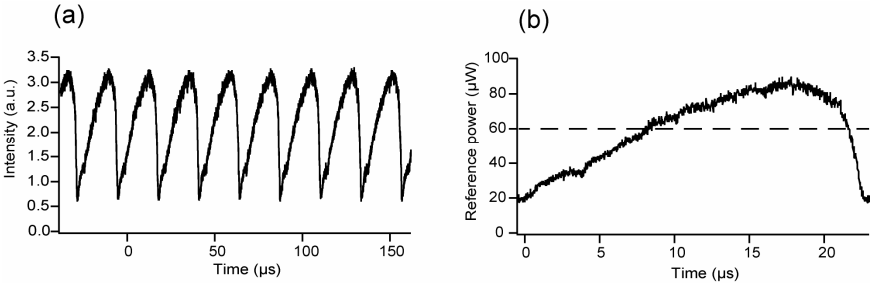

Fig. 2. (a). Wavelength-swept laser output characteristics. Oscilloscope trace shows 43.2-kHz sweep rate. (b). Instantaneous optical power in the reference arm.

The 800-nm OFDI system has been described previously in detail [20]. In this work, we have modified the system for retinal imaging (Fig. 3). The average output power at a SOA injection current of 140 mA was 7 mW. The beam from the laser source is attenuated so that the interferometer is illuminated with 1.3 mW. The reference arm (70%) has a translational delay and a neutral-density (ND) filter that attenuates the reference beam power further. A fraction of laser beam (30%) is guided to a slit-lamp in the sample arm. Data was acquired with a high-speed digitizer (National Instruments, PCI-5122) at a sampling rate of 50 Ms/second (14-bit resolution). During each wavelength sweep, 1024 data points were sampled over 20.5 μs (duty cycle of 88%). Post-processing of the acquired data involves a series of steps, details of which were described previously [5, 6, 19]. For the apodization step, we used a bell-shaped window function that falls off sinusoidally over 200 data points at both ends.

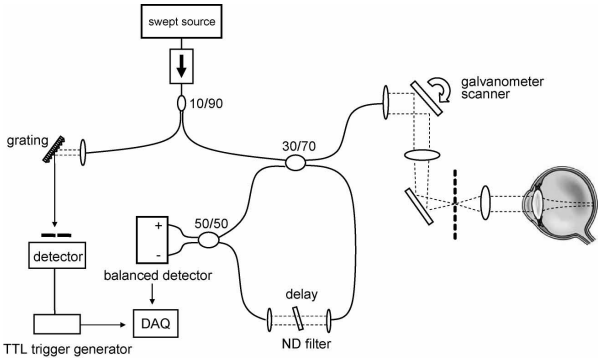

Fig. 3. Experimental configuration of the optical frequency domain imaging system.

To confirm equivalent performance with our circular cavity design [20], the sensitivity and axial resolution of the OFDI imaging system with the linear cavity was characterized by placing a mirror in the sample arm consisting of a collimator and a mirror, and varying the delay in the reference arm [Fig. 4(a)]. The optical power at the fiber end in the sample arm was 460 μW, which was attenuated with a ND filter (single pass OD = 2.5). The sum of the power arriving at each port of the 50/50 coupler immediately before the balanced detector was 2.2 nW. The optimal reference arm power was 60 μW [20]. The reflectivity peaks as a function of path length delay between sample and reference arm were fitted with a Gaussian. The coherence length, defined as the length at which the interference amplitude decreases by a factor of 2, corresponding to a 6-dB sensitivity reduction, is 2.0 mm, in agreement with the TF linewidth of 0.07 nm. We did not observe any significant artifact that could arise from formation of a parasitic Fabry-Perot cavity. A peak sensitivity of 91 dB was achieved at a

#74442 - $15.00 USD Received 29 August 2006; revised 4 December 2006; accepted 5 December 2006

sample arm power of 460 μW, which is 12 dB lower than the theoretical shot-noise limited value [9, 15]. We reported a comparable result in the previous study [20] where the peak sensitivity of the OFDI system was 11 dB lower than the shot-noised limited (96-dB peak sensitivity at 2.4-mW sample arm power). A further analysis of the noise contributions indicate that the combination of data acquisition board (National Instruments, PCI-5122) noise and detector (New Focus, 1807-FS) thermal noise at a frequency of 5 MHz is twice the lowest noise specified for the detector. As a result, at 60-μW reference power the shot noise is equal to the thermal noise contribution. At power levels above 60 μW, relative intensity noise (RIN) of the laser starts to dominate despite the balanced detection. From a measurement with an unbalanced detector the RIN at 60-μW reference arm power was estimated to be 18 dB larger than the shot noise or thermal noise, consistent with our earlier estimate of 18-dB RIN suppression under the assumption of a lower thermal noise [20]. The combined effect of thermal and RIN contributes 3-5 dB sensitivity degradation with respect to shot noise limited detection. Secondly, for calculating the shot-noise limited sensitivity we assume a constant reference arm power. Apparently this is not the case in our system; the laser output power varies as the wavelength is tuned from short to long wavelengths, hence the optical power in the reference arm follows the trace of Fig. 2(b). The flat-spectrum approximation underestimates the thermal and RIN contribution that are present in the system. Only at the wavelengths where the source power is equal to the average power [*i.e.* intersections between the instantaneous power and the mean power in Fig 2(b)] the optimal sensitivity is achieved. For wavelengths were the instantaneous power is higher or lower than the average power, the sensitivity is further degraded from RIN or thermal noises, respectively. We estimate that this effect could cause a 3-5 dB reduction in the sensitivity. Thirdly, RIN is not completely suppressed over the entire wavelength range, because of wavelength-dependent coupling ratio of the nominal 50/50 splitter. Additional loss arises from wavelength-dependent polarization mismatch between the sample and reference beams, and also from the apodization step in post-processing, which we estimate to be of equal magnitude. The latter gives rise to 1-dB SNR degradation. After sampling and windowing of measured spectra, an axial resolution of 13-13.5 μm in air was achieved across a depth range of 3 mm [Fig. 4(b)]. Mapping inaccuracies and uncompensated dispersion in the interferometer may have contributed to the small axial resolution degradation as a function of depth.

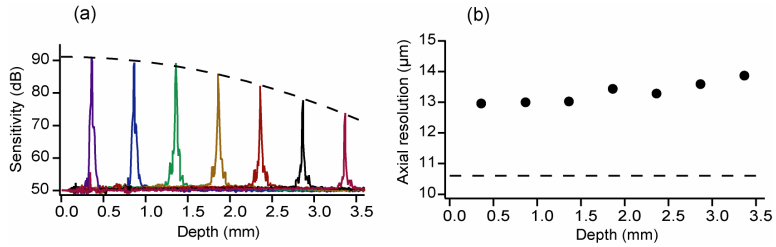

Fig. 4. (a). Sensitivity as a function of depth. (b). Axial resolution in air as a function of depth. Dashed line is the theoretical axial resolution calculated from the raw laser spectrum.

3. Results

The sample arm of the interferometer was connected to a slit lamp based human interface that was described in detail previously [5, 6, 11]. An undilated eye of a healthy volunteer was illuminated with 460 μW, in compliance with ANSI standards for pulsed illumination [23]. Two regions of interest were imaged, one centered at the fovea (Fig. 5) and the second visualizing both the ONH and the fovea (Fig. 6). The still images of Figs. 5 and 6 consisted of 1024 A-lines. Figure 3 is an image of a macular region that is cropped to 950 x 250 pixels (6.4 mm x 1.4 mm in tissue). The visualized features correlate well with the known retinal layers. Figure 6 is a representative tomogram of an area that includes the optics nerve head and fovea (6.4 mm x 1.9 mm in tissue).

#74442 - $15.00 USD Received 29 August 2006; revised 4 December 2006; accepted 5 December 2006

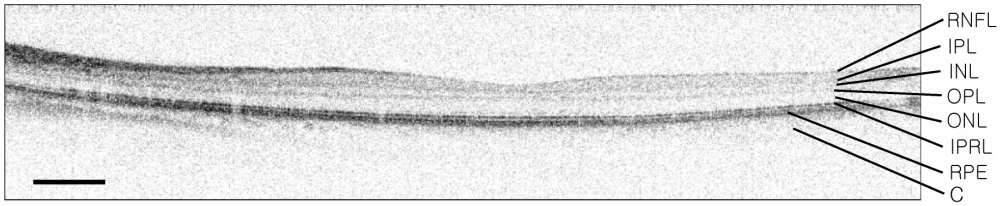

Fig. 5. Macular region, 6.4 mm wide X 1.4 mm deep (in tissue). Scale bar, 500 μm. RNFL: retinal nerve fiber layer. IPL: inner plexiform layer. INL: inner nuclear layer. OPL: outer plexiform layer. ONL: outer nuclear layer. IPRL: inner photoreceptor layer. RPE: retinal pigment epithelium. C: choroids.

For the movies (for links in Figs. 5 and 6), the lateral scan speed was doubled, such that movie frames consisted of 512 A-lines. The movies display a scan over a transverse area of 6.1 mm x 3.5 mm, and the axial ranges (in tissue) of each movie frame are 1.4 mm (linked to Fig. 5) and 1.9 mm (linked to Fig. 6), respectively. Sequences of 180 frames were acquired at 84 frames per second (fps), and compiled into movies that play back at 30 fps. Scans of the whole transverse area took about 2.13 seconds.

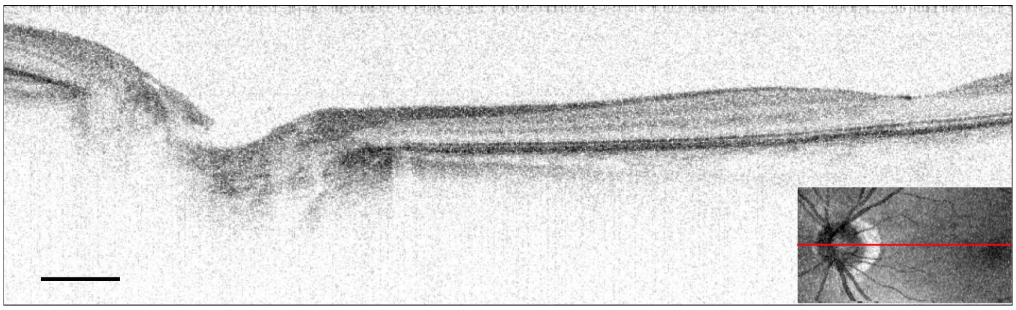

Fig. 6. Area that includes optic disk and fovea, 6.4 mm wide X 1.9 mm deep (in tissue). Scale bar, 500 μm. Inset; en face image with a red line whose cross section is shown in the left, 6.4 mm X 3.5 mm.

An *en face* view (Fig. 6, inset) is constructed by integrating the scanned 3-D volume over the axial dimension and shows the exact location of the OCT scan on the *en face* reconstruction.

4. Conclusion

We have described imaging of human retina *in vivo* with swept-source OCT. The peak sensitivity is 91 dB at an A-line rate of 43,200 per second and with an optical power of 460 μW in the sample arm. The axial resolution in air is 13-13.5 μm with a ranging depth of 2 mm. A volumetric scan of 180 individual frames covering a 21^o x 12^o (6.1 x 3.5 mm^2) field-of-view was acquired in 2.13 sec. This represent the fastest, wide field-of-view, volumetric retinal OCT imaging with a superior ranging depth over SD/FD-OCT technology, however at the cost of a 3.5 fold reduction in axial resolution [11, 12]. Further speed increases are not limited by the laser sweep repetition rate, but by the sensitivity penalty associated with increased A-line rate. However, the developments in ophthalmic instrumentation, such as wavefront correction with adaptive optics [24-27] could provide the extra sensitivity permitting a further speed increase. Future system improvements to recover a portion of the 12 dB difference between shot-noise limited and experimentally achieved sensitivity could also be used to increase the imaging speed.

#74442 - $15.00 USD Received 29 August 2006; revised 4 December 2006; accepted 5 December 2006

Acknowledgments

This research was supported in part by research grants from the National Institutes of Health (R01-RR019768 R01-EY014975) and the Department of Defense (F4 9620-01-1-0014).

#74442 - $15.00 USD Received 29 August 2006; revised 4 December 2006; accepted 5 December 2006